Introduction

Authors Alfred G. Emslie, Francis T. Bonner and Leslie G. Peck predict the fluid distribution on a rotating disc as a function of time and space for any radially symmetric initial distribution using fundamental transport equations. Many coating applications from varnishes to microelectronics call for a uniform film of a specific thickness which can be manufactured by the centrifugation of liquid material followed by drying or solidification. The film contour on a centrifuge disc changes in space and time as a result of the viscous and centrifugal forces acting on the fluid, which are fundamentally dependent on fluid viscosity and plate angular speed. A theoretical model presented by the authors quantifies the relative strength of these forces for a fluid of choice, thereby providing a set of operating conditions to produce a desired film. For example, if the fluid of choice is a paint with a known viscosity, an initial contour of material can be morphed in different ways by adjusting the angular speed and the duration of the centrifugation. The model set forth by the authors takes the hypothetical operating conditions as parameters and delivers the fluid contour outcome.

This review is composed of a review of the methods used in the original publication with additional connections to the fundamental transport equations, followed by the presentation of the solutions built into a node-network profile simulator produced in Microsoft Excel ™. This node network demonstrates the fluid contour profile as it distorts upon the commencement of centrifugation for nearly any conceivable initial condition, with example contours presented. Concluding remarks summarize the findings of this review.

Methods

First, a broad overview of the methods is presented followed by a more detailed recap. The authors created a mathematical model for the radial fluid profile on a rotating plate by applying several simplifying assumptions to the transport equations. The result of the transport equation is a relationship between the viscous and centrifugal forces using the force-flux relationship of a viscous Newtonian fluid and the circular motion body force. The integration of the transport equation produces a radial velocity function. The radial velocity has a direct effect on the fluid height because as material flows outward, the height of fluid must sink for a fixed amount of initial material. The dependent height profile is found by combining the radial velocity function with the flow form of the continuity equation to satisfy conservation of mass for a fluid of constant density. The resultant fluid height equation is a nontrivial partial differential equation (PDE). The authors connected this PDE with a total differential for h, which included many of the same terms. Therefore, the PDE was split into two ordinary differential equations (ODE), one for vertical position and one for radial position. These can are integrated with the initial condition that the initial position is equal to a constant at the beginning of the time interval. See the appendix for a detailed, step-by step derivation.

The authors derive a mathematical model for fluid contour on a rotating plate by applying several simplifying assumptions and balance equations. Table 1 presents paraphrased statements of the authors' simplifying assumptions set forth at the start of their work to define the validity range and limitations of their model.

Table 1: Fundamental Analysis Assumptions

	Foundational Assumptions
1	Semi-infinite flat plate (the plate radius is larger than the outermost extent of fluid)
2	Gravitational forces are negligible compared to centrifugal forces (the plate spins fast)
3	Radially symmetric initial (and transient) fluid distribution
4	Viscosity is independent of shear rate (Newtonian Fluid)
5	Shear resistance is only significant in horizontal planes (relatively thin layers)
6	Radial velocity is sufficiently low to neglect Coriolis forces.
7	The top of the fluid film is exposed to air which exerts negligible shear forces.

Although the authors begin with Equation 2 as a force balance between viscous and centrifugal forces, Equation 2 can be derived from the radial component of the cylindrical transport equation, Equation 1, where the gravitation body force term has been replaced by a centrifugal body force term. No pressure gradient is present and in the reference frame of the moving plate, the material derivative is zero. Additionally, assumption 4 in Table 1 can be applied yielding Equation 2. The fluid density, viscosity, radial velocity, radial position and axial position are given by ρ, μ, v_r, r and z, respectively.

$$\rho\left(\frac{Dv}{Dt}\right) = -\nabla P - (\nabla \cdot \tau) + \rho(\omega^2 r) \quad (1)$$

$$-\mu\left(\frac{\partial^2 v_r}{\partial z^2}\right) = \rho(\omega^2 r) \quad (2)$$

Integrating Equation 2 twice with boundary conditions according to the methods presented in Section 2.2 in "Transport Phenomena" by Bird, Steward and Lightfoot gives Equation 3. The boundary conditions are (1) that the radial velocity is zero at the plate-fluid interface, also referred to as the "no-slip condition", and (2) the fluid at the air-fluid interface experiences zero shear stress, despite the changing height of the fluid.

$$v_r = \frac{\rho(\omega^2 r)}{\mu}\left(-\frac{z^2}{2} + hz\right) \quad (3)$$

Equation 3 describes the radial velocity, but the height of the fluid is not constant (this is the main purpose of the problem) but height and radial velocity are connected by means of conservation of mass as given by the continuity equation. For a fluid of constant density, the continuity equation in terms of volumetric flow, q, is used as written in Equation 4 to couple the height of the fluid film in connection with the radial flow of material.

$$r\frac{\partial h}{\partial t} = \frac{\partial(rq)}{\partial \mathrm{r}} \quad (4)$$

An expression for the volumetric flow rate is obtained by integrating Equation 3 with respect to z from 0 to h. Inserting the product into Equation 4 produces Equation 5.

$$\frac{\partial h}{\partial t} = -\frac{\rho(\omega^2)}{3\mu r}\frac{\partial}{\partial r}(r^2 h^3) \quad (5)$$

Applying the chain rule to the right-hand side of Equation 5 and rearranging gives the PDE presented in Equation 6.

$$\frac{\partial h}{\partial t} = \frac{2\rho(\omega^2)h^3}{3\mu} - \frac{3\rho(\omega^2)rh^2}{3\mu}\frac{\partial h}{\partial r} \quad (6)$$

The authors solve this nontrivial PDE by identifying that the equation resembles the total derivative for h given in Equation 7.

$$\frac{dh}{dt} = \frac{\partial h}{\partial t} + \frac{\partial h}{\partial r}\frac{dr}{dt} \quad (7)$$

Mutual consistency of Equations 6 and 7 requires that Equations 8 and 9 are true. The result of the mutual consistency is the combination of a PDE with a total differential to produce two ODEs, Equation 8 and Equation 9, which are much easier to use.

$$\frac{dh}{dt} = -\frac{2\rho(\omega^2)h^3}{3\mu} \quad (8) \qquad\qquad \frac{dr}{dt} = \frac{\rho(\omega^2)rh^2}{\mu} \quad (9)$$

Equations 8 and 9 can be integrated with application of the initial height and position of a given fluid particle at time zero to yield Equation 11 and Equation 12, respectively. Furthermore, the authors introduce a constant, K, in Equation 10 to simplify Equation 11 and Equation 12. Equation 11 and 12 are the framework for the solution set presented by the authors and used in the analysis that follows.

$$K = \frac{4\rho(\omega^2)}{3\mu} \tag{10}$$

$$h = \frac{h_o}{\left(Kh_o^2 t + 1\right)^{\frac{1}{2}}} \tag{11}$$

$$r = r_o\left(Kh_o^2 t + 1\right)^{\frac{3}{4}} \tag{12}$$

Results and Discussion

The solutions presented by the authors in Equations 11 and 12 provide a coupled set of equations to describe the position of a fluid particle in space and time on a rotating disc. Therefore, combining many "nodes", the macroscopic fluid profile can be thoroughly studied. This work includes a simulator that takes fluid properties as parameters, which gives the fluid profile as a function of space and time. The "node" network approach allows straightforward tracking of fluid elements, located at each vertex in the mesh, as the fluid elements migrate upon subjection to the forces. Figure 1 shows the contortion of an arbitrary cylindrical initial contour.

The centrifugal force increases with increasing distance away from the axis of rotation, while the viscous force increases with increasing proximity to the rotating plate. Therefore, fluid in the upper right extreme of Figure 1 migrates the most in this instance. Conservation of mass requires that material near the center settles to a lower height to fill nearby voids. Notably, the 'no slip' condition remains in effect at the plate surface. The areas in between experience a combination of the forces, resulting in the observed node network deformation. An important note is that conservation of volume occurs for the system, not conservation of profile area. In the profiles shown in Figures 1 and 2, a rotated cross-section of a given section of the mesh about the vertical axis results creates a different volume based on distance from the center of rotation.

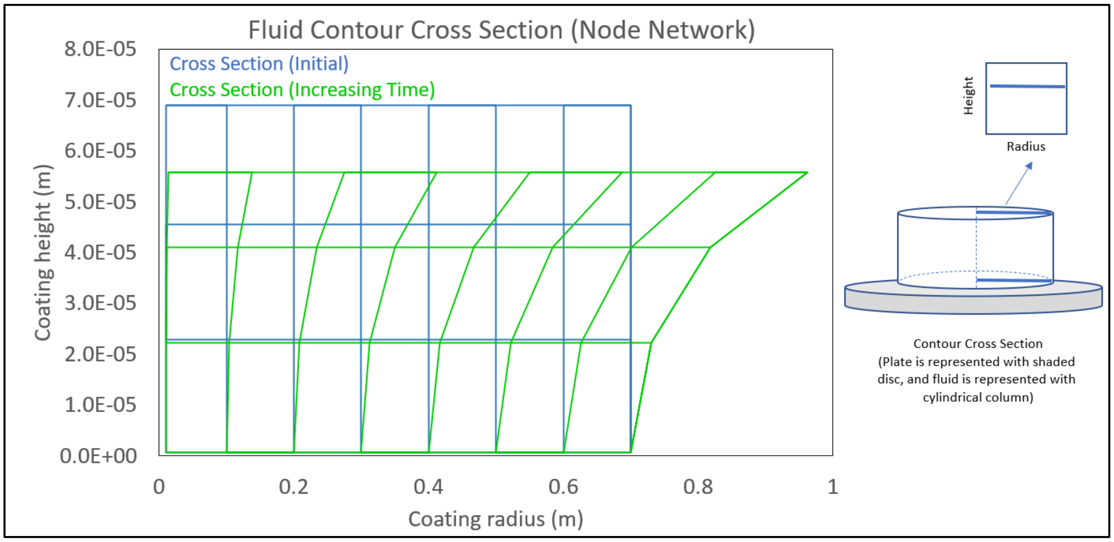

Figure 1: Node network excel simulator profile (left). A schematic (right) demonstrates context for the plot. The center of the disc is at the origin of the plot, and the vertical axis represents the height of a fluid particle in the axial direction and the horizontal axis depicts the radial position from the center of rotation. Equations 13 and 14 are applied to 28 different locations in a fluid, the time dependent response is shown from the initial location (blue) to the location of the network at time thereafter. The model fluid in this case has the properties of honey.

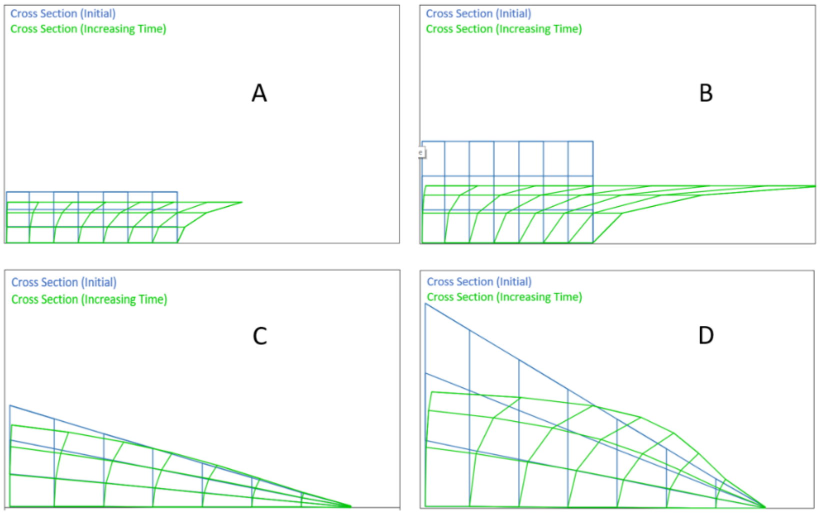

A uniform initial height produces a uniform final height, while a non-uniform initial height produces a transient profile response where many shapes are possible. The apparatus studied is most commonly used for films of uniform thickness as shown in Figure 1, but additional gradient profiles can be created such as the cone profile in Figure 2 D which can be spun into a film with a desired pitch.

Figure 2: Sample contours for a fluid with the properties of honey, with an arbitrary height of 0.3mm and radius 0.7m. Doubling the height of a given initial uniform distribution results in more than double the horizontal displacement of the fluid, as noted by (B) compared to (A). Similarly, doubling the height of a cone-shaped initial distribution results in significantly increased contortion, demonstrating that centrifugal forces become increasingly more important as vertical distance from the plate increases.

Conclusion

The publication by Emslie, Bonner and Peck helped to expedite the prediction process for liquid spin coating. The mathematical model set forth based on first principles ultimately predicts the position of a fluid particle in cylindrical space as a function of time and the properties of the fluid. Most importantly, this prediction provides a preliminary estimate for a manufacturer as to what rotation speed and duration should be used for a particular fluid to obtain a desired film contour. Machines are becoming increasingly sophisticated, but the laws of fluid mechanics described by fundamental transport equations remain unchanged. In more recent years, polymer spin coating has become more complicated with the onset of new polymers that are non-Newtonian fluids. It is noteworthy to mention that the analysis used in this work was produced according to the assumptions set forth in Table 1, and therefore the accuracy of this model depends upon the degree of validity of the assumptions.

This review of the publication of interest has been insightful on several fronts. The transport equations include relevant forces acting on a spinning fluid, and the magnitude of these forces is significant. Gravitational forces are neglected due to the large magnitude of centrifugal and viscous forces, which means that the solution presented herein will only be valid for large angular speeds relative to gravity, which is practical because manufacturers can easily produce a rapidly spinning disc and cannot afford painfully slow speeds anyway. Not surprisingly, the centrifugal forces dominate the fluid farthest from the plate, while the viscous forces prevent almost all motion near the plate surface. It should be noted that a boundary layer theory model would be necessary to accurately capture the behavior of a relatively thick or low-viscosity film.

The authors present several initial fluid distributions and predict the outcome as a function of time and space. Although these predictions are limited to radially symmetric starting conditions, this is relevant to industry because a dispenser can add fluid to a plate in a location any distance from the center in radially symmetric patterns upon disc rotation, such as the sinusoidal distribution presented by the authors, or the cone shaped profile included in this work.

References

Publication upon which the study is based:
Emslie, Bonner and Peck, 1958. "Flow of a viscous liquid on a rotating disc" *Journal of Applied Physics*, Volume 29, Number 5, May 1958

Transport Textbook
Bird, Stewart and Lightfoot, 2007 "Transport Phenomena: Revised Second Edition", *John Wiley and Sons, Inc.*

Density and Viscosity of Honey:
Oroian, Mircea, 2020. "Measurement, prediction and correlation of density, viscosity, surface tension and ultrasonic velocity of different honey types at different temperatures", *Journal of Food Engineering*, Volume 119, Issue I, November 2013, Pages 167-172. Accessed through Science Direct via Measurement, prediction and correlation of density, viscosity, surface tension and ultrasonic velocity of different honey types at different temperatures - ScienceDirect

Functional paint viscosity
2020 "Optimum viscosity for paint application", American Coatings Association, accessed via Optimum Viscosity for Paint Application - American Coatings Association

Appendix: Full solution

Equation of motion, cylindrical coordinates

$$\rho\left(\frac{Dv}{Dt}\right) = -\nabla P - (\nabla\cdot\tau) + \rho g$$

$$F_{gv} = \rho g$$ Gravitational body force

$$F = ma$$

$$F_g = mg$$

$$F_{cv} = \rho(\omega^2 r)$$ Centrifugal body force

$$F_c = m\left(\frac{v^2}{r}\right)$$

$$F_c = m(\omega^2 r)$$

$$\rho\left(\frac{Dv}{Dt}\right) = -\nabla P - (\nabla\cdot\tau) + \rho(\omega^2 r)$$ Body forces: use F_{cv} instead of F_{gv}

$$\rho\left(\frac{Dv}{Dt}\right) = -\nabla P + \mu\nabla^2 v + \rho(\omega^2 r)$$ Newtonian Fluid with constant density

$$-\mu\left(\frac{\partial^2 v_r}{\partial z^2}\right) = \rho(\omega^2 r)$$ Reference frame of moving plate as v = 0
Negligible Pressure gradient

$$-\mu\left(\frac{\partial^2 v_r}{\partial z^2}\right) = \rho(\omega^2 r)$$ Integrate

$$\frac{\partial}{\partial z}\left(\frac{\partial v_r}{\partial z}\right) = -\frac{\rho(\omega^2 r)}{\mu}$$

$$\int \partial\left(\frac{\partial v_r}{\partial z}\right) = -\int \frac{\rho(\omega^2 r)}{\mu}\partial z$$

Boundary Conditions

$$\frac{\partial v_r}{\partial z} = 0 \quad @ \quad z = h$$

$$\frac{\partial v_r}{\partial z} = -\frac{\rho(\omega^2 r)}{\mu} z + C_1$$

$$0 = -\frac{\rho(\omega^2 r)}{\mu} h + C_1$$

$$C_1 = \frac{\rho(\omega^2 r)}{\mu} h$$

$$\int \partial v_r = -\int\left(\frac{\rho(\omega^2 r)}{\mu} z + C_1\right)\partial z$$

$$v_r = -\frac{\rho(\omega^2 r)}{2\mu} z^2 + C_1 z + C_2$$

$$v_r = 0 \quad @ \quad z = 0$$

$$0 = 0 + 0 + C_2$$

$$C_2 = 0$$

$$v_r = -\frac{\rho(\omega^2 r)}{2\mu} z^2 + \frac{\rho(\omega^2 r)}{\mu} hz$$ Sub in C_1 and C_2

$$v_r = \frac{\rho(\omega^2 r)}{\mu}\left(-\frac{z^2}{2} + hz\right)$$ Rewrite to simplify

$$v_r = \frac{\rho(\omega^2 r)}{\mu}\left(-\frac{z^2}{2} + hz\right)$$

$$q = \int_0^h v_r dz$$

$$q = \frac{\rho\omega^2 r h^3}{3\mu}$$

$$r\frac{\partial h}{\partial t} = \frac{\partial(rq)}{\partial r}$$

$$\frac{\partial h}{\partial t} = -\frac{\rho(\omega^2)}{3\mu r}\frac{\partial}{\partial r}(r^2h^3)$$

$$\frac{\partial}{\partial r}(r^2h^3) = h^3\frac{\partial}{\partial r}(r^2) + r^2\frac{\partial}{\partial r}(h^3)$$

$$\frac{\partial h}{\partial t} = \frac{2\rho(\omega^2)h^3}{3\mu} - \frac{3\rho(\omega^2)rh^2}{3\mu}\frac{\partial h}{\partial r}$$ PDE

$$-\frac{2\rho(\omega^2)h^3}{3\mu} = \frac{\partial h}{\partial t} + \frac{\rho(\omega^2)rh^2}{\mu}\frac{\partial h}{\partial r}$$ Rearrange

$$\frac{dh}{dt} = \frac{\partial h}{\partial t} + \frac{\partial h}{\partial r}\frac{dr}{dt}$$ Use total derivative definition

$$\frac{dh}{dt} = -\frac{2\rho(\omega^2)h^3}{3\mu} \qquad \frac{dr}{dt} = \frac{\rho(\omega^2)rh^2}{\mu}$$ 2 ODEs from 1 PDE

$$\int\frac{1}{h^3}dh = -\frac{2\rho(\omega^2)}{3\mu}dt$$

$$\frac{-0.5}{h^2} = -\frac{2\rho(\omega^2)}{3\mu}t + C_1$$

Boundary Condition

$h = h_o$ @ $t = 0$

$$\frac{-0.5}{h_o^2} = C_1$$

$$\frac{-0.5}{h^2} = -\frac{2\rho(\omega^2)}{3\mu}t - \frac{0.5}{h_o^2}$$ Sub in C_1

$$\frac{-0.5}{1} = h^2\left(-\frac{2\rho(\omega^2)}{3\mu}t - \frac{0.5}{h_o^2}\right)$$

$$\frac{-0.5}{\left(-\frac{2\rho(\omega^2)}{3\mu}t - \frac{0.5}{h_o^2}\right)} = h^2$$

$$h^2 = \frac{1}{\left(\frac{4\rho(\omega^2)}{3\mu}t + \frac{1}{h_o^2}\right)}$$

$$h^2 = \frac{h_o^2}{\left(\frac{4\rho(\omega^2)h_o^2}{3\mu}t + 1\right)}$$

$$h = \frac{h_o}{\left(\frac{4\rho(\omega^2)h_o^2}{3\mu}t + 1\right)^{1/2}}$$

Solution for axial fluid position

$$\frac{dr}{dt} = \frac{\rho(\omega^2)rh^2}{\mu}$$

ODE for r

$$\frac{dr}{dt} = \frac{\rho(\omega^2)rh_o^2}{\mu\left(\frac{4\rho(\omega^2)h_o^2}{3\mu}t + 1\right)}$$

$$\int \frac{1}{r}dr = \int \frac{\rho(\omega^2)h_o^2}{\mu\left(\frac{4\rho(\omega^2)h_o^2}{3\mu}t + 1\right)}dt$$

$$A = \frac{\rho(\omega^2)h_o^2}{\mu} \qquad B = \frac{4\rho(\omega^2)h_o^2}{3\mu}$$

$$\int \frac{1}{r}dr = A\int \frac{1}{(Bt + 1)}dt$$

$$\ln(r) = \frac{A}{B}\ln(Bt + 1) + C_1$$

Boundary Condition

$$r = r_o \quad @ \quad t = 0$$

$$\ln(r_o) = C_1$$

$$C_1 = \ln(r_o)$$

$$\ln(r) = \frac{A}{B}\ln(Bt + 1) + \ln(r_o)$$

Sub in C_1

$$\frac{\ln(r)}{\ln(r_o)} = \frac{A}{B}\ln(Bt + 1)$$

Rearrange

$$\frac{r}{r_o} = (Bt + 1)^{\frac{A}{B}}$$

$$r = r_o\left(\frac{4\rho(\omega^2)h_o^2}{3\mu}t + 1\right)^{3/4}$$

Solution for radial fluid position

PDE Solution Summary

$$\frac{\partial h}{\partial t} = \frac{2\rho(\omega^2)h^3}{3\mu} - \frac{3\rho(\omega^2)rh^2}{3\mu}\frac{\partial h}{\partial r}$$ PDE

$$-\frac{2\rho(\omega^2)h^3}{3\mu} = \frac{\partial h}{\partial t} + \frac{\rho(\omega^2)rh^2}{\mu}\frac{\partial h}{\partial r}$$ Rearrange

$$\frac{dh}{dt} = \frac{\partial h}{\partial t} + \frac{\partial h}{\partial r}\frac{dr}{dt}$$ Use total derivative definition

$$\frac{dh}{dt} = -\frac{2\rho(\omega^2)h^3}{3\mu} \qquad \frac{dr}{dt} = \frac{\rho(\omega^2)rh^2}{\mu}$$ 2 ODEs from 1 PDE

$$h = \frac{h_o}{\left(\frac{4\rho(\omega^2)h_o^2}{3\mu}t + 1\right)^{1/2}} \qquad r = r_o\left(\frac{4\rho(\omega^2)h_o^2}{3\mu}t + 1\right)^{3/4}$$

ODE Solutions for

$h = h_o$ @ $t = 0$

$r = r_o$ @ $t = 0$

$$h = \frac{h_o}{(Kh_o^2t + 1)^{1/2}} \qquad r = r_o(Kh_o^2t + 1)^{3/4} \qquad K = \frac{4\rho(\omega^2)}{3\mu}$$